DEPARTMENT OF THE INTERIOR

U.S. GEOLOGICAL SURVEY

Application of Spiking and Predictive Deconvolution to Short Record Length Reflection Data

by

Robert A. Williams[1] and Kenneth W. King[1]

Open-File Report 86-299

[1]U.S. Geological Survey
Golden, Colorado

PREFACE

The deconvolution process is the method by which the filtering (convolution) effect of the earth and the input seismic source pulse are separated (deconvolved). The removal of the earth's filter from the source wavelet restores this wavelet to a form that is nearly the same it had before it was filtered by the earth; i.e., it is shorter in length and it more closely resembles a spike (if one is working with impulsive sources). This contracted, higher frequency wavelet permits greater resolution in the processed data which is important in engineering seismology where the targets are very shallow and the strata may be very thin.

The two types of deconvolution filtering used in this study, spiking and predictive, are variations of the Wiener filtering process. Norbert Wiener developed his filter theory in the late 1940's, and the principal ideas of his work were quickly adapted to the seismic data processing industry. Using the recorded seismic data and the Wiener filter process one can determine a filter that is the inverse of the seismic pulse, which has been distorted by the earth filter. This inverse filter is then applied to the field data to remove the effects of the distorting earth filter. Spiking deconvolution attempts to produce a spike or impulse at each reflection point in the field data. However, due to noise present in the data, the algorithm that designs the inverse filter develops some errors and thus the output diverges from the desired spike. Predictive deconvolution, on the other hand, does not attempt to output a spike. Rather, it is designed to preserve the waveform (as recorded in the field) up to a certain time called the prediction distance. It then acts on the latter part of the waveform to remove distortions in the seismic pulse created by filtering in the earth.

CONTENTS

Page

Preface i
Abstract 1
Introduction 1
Field site geology 2
Field methods 2
Seismic data processing 2
Source signature 7
Results 9
  Pre-stack versus post-stack deconvolution 9
  Time shifting of events 15
  Filter lengths 15
  White noise tests 15
  Zero-phase filtering 15
  Post-deconvolution bandlimiting filter 20
  Subsurface modeling 20
Conclusions 23
References 23

ILLUSTRATIONS

Figure 1. Location map of the Denver Federal Center 3
2. Interval velocities calculated from downhole work at the Denver Federal Center 4
3. Amplitude spectra for two unprocessed traces of cdp 148 5
4. Unprocessed cdp gathers; same cdp gathers with nmo, mute, and filter applied 6
5. Betsy 8-gauge source signature 8
6. Results of spiking and gap deconvolution filtering applied prior to stacking 10
7. Results of spiking and gap deconvolution filtering applied after stacking 11
8. Spectral analysis for one stacked cdp using spiking deconvolution before and after stacking 12
9. Spectral analysis comparison of one stacked cdp using gap deconvolution before and after stacking 13
10. Comparison of time shifting of reflection events for spiking deconvolution applied before and after stacking 14
11. Results of using spiking deconvolution after stacking with and without adding white noise 16
12. Results of using gap deconvolution after stacking with and without adding white noise 17
13. White noise level tests using spiking deconvolution filtering applied before stacking 18
14. Zero-phase filtering effects on spiking deconvolution 19
15. Results of using zero-phase filtering after deconvolution 21
16. Comparison of synthetic stack to real stacked data 22

TABLE

Table 1. Processing sequence and field parameters 7

APPLICATION OF SPIKING AND PREDICTIVE DECONVOLUTION TO SHORT RECORD LENGTH REFLECTION DATA

by

Robert A. Williams and Kenneth W. King

ABSTRACT

Tests of two types of Wiener filtering, predictive and spiking, on short record length (100 ms) reflection field data show that large changes in added white noise have little degrading effect on stack quality when applying deconvolution after stacking the data. However, when deconvolving the data before stacking, increasing the white noise level produced noticeable improvement in stack quality. Large variations in deconvolution filter operator length displayed minor differences in stack quality when deconvolving both before and after stacking. Deconvolving after stacking, versus before stacking, showed dramatic improvement in several categories: resolution, high-frequency enhancement, spectral broadening and spectral balancing within the bandlimited region. A test of the post-deconvolution bandlimiting filter demonstrated that its application was more helpful to stack quality when it followed the spiking filter as compared to following the predictive filter. Additional results showed that the spiking deconvolution filter caused a greater time shift of reflections than the predictive filtering; and applying a zero-phase band pass filter before deconvolution gave better results (with both spiking and predictive filtering) than not using this filter.

INTRODUCTION

Wiener filtering is generally the most common method of deconvolution used in the seismic data processing industry. The method has proven to be quite reliable in terms of its goals: (1) to equalize the spectrum; (2) to whiten the spectrum; and (3) to improve resolution. The purpose of this paper is to test the performance of two types of Wiener filtering, spiking and predictive (gap), on short data lengths. Both types are predictive except that the prediction distance for spiking is equal to 1. Throughout this paper the form of predictive deconvolution, where the prediction distance varies, is referred to as "gap." The short data lengths are primarily for engineering geology applications where the depths to targets are in tens of feet. The type of low-energy/high-frequency seismic source used in this report is the 12-gauge shotgun. The reflective seismic data generated by this source is difficult to interpret before stack because the induced reflective energy is filled with coherent and incoherent noise. The performance of Wiener filtering in the presence of this noise is tested in several ways by using the same data set throughout all tests. Variable input parameters, such as the white noise level and deconvolution filter operator length, are tested on this noisy data set. Other properties of deconvolution such as its response to zero-phase filtering before and after deconvolution are tested. The results of this study may be applicable to other shallow reflection data that have a low signal-to-noise ratio.

FIELD SITE GEOLOGY

The U.S. Geological Survey collected the data used in this paper on the southeast side of the Denver Federal Center in Lakewood, Colo. (fig. 1). Two borings drilled 10 ft from the seismic reflection line provided geologic information down to a 60-ft depth. These borings revealed the shallow subsurface to be mainly alternating sand, sandstone, silt, and clay layers ranging in thickness from 1 to 3 ft. Most layers are consolidated with a few thin lithified units. Refraction data along the seismic reflection line, corroborated by well information, indicate a strong velocity contrast (1,200- to 5,000 ft/s) at a depth of 12 ft (fig. 2). This velocity contrast corresponds to the depth of an aquitard (saturated layer); samples below this layer in the borings were all dry. The thickness of the slower velocity layer averages approximately 12 ft which translates to 20-ms two-way traveltime on the reflection data.

FIELD METHODS

The line is straight and flat with no elevation changes. An Input/Output, Inc., DHR-2400, 24-channel system recorded the data. Single geophones were used at each station and spaced 5 ft apart. Near source offset was 10 ft and the farthest was 65 ft. The source interval was 5 ft. Two shots were fired at each station for the entire line. The source was returned to the beginning of the line and shot again at two shots per station with the same configuration except that each station had been moved one-half station interval. The 80-Hz low-cut filter used during recording reduced ground-roll energy. Records of 250-ms duration with a 0.25-ms sampling period were generated. The upper 100 ms were used in the deconvolution tests described in this paper.

The 12-gauge shotgun fired 1-oz lead slugs vertically down the barrel of a "Betsy Seisgun." Baffles and a steel base plate at the end of the barrel helped reduce the air waves and stabilize the gun. The shotgun source generated frequencies in the 50- to 450-Hz range at this site. The dominant frequencies at about 100 Hz (fig. 3) are due to a strong ground-coupled air wave. The air wave unfortunately contributes a significant amount of energy around 100 Hz, which easily saturates the recording system and inhibits the recording of weaker reflection energy.

SEISMIC DATA PROCESSING

The shooting pattern with a two-shot summation generated 24-fold common-depth-point (cdp) data with a subsurface sampling interval of 2.5 ft. Normal-moveout correction (nmo), which is applied to the cdp gathers, dynamically adjusts the cdp traces in time to a position that represents a normal incidence traveltime to a reflector interface. Nmo followed editing and sorting into cdp gathers. Muting of traces zeroes the amplitudes of unwanted seismic energy within a time interval specified by the processor. Muting followed nmo and was used to help build the signal-to-noise ratio by eliminating unwanted pre-first arrival noise and part of the air wave (fig. 4). Later tests of zero-phase band-pass filters applied to the data prior to deconvolution filtering indicated that it was a desirable procedure for this data set. Unless otherwise stated in the text, the pre-deconvolution zero-phase band-pass filter (-3 dB corners at 200 and 250 Hz, and -18 dB/octave

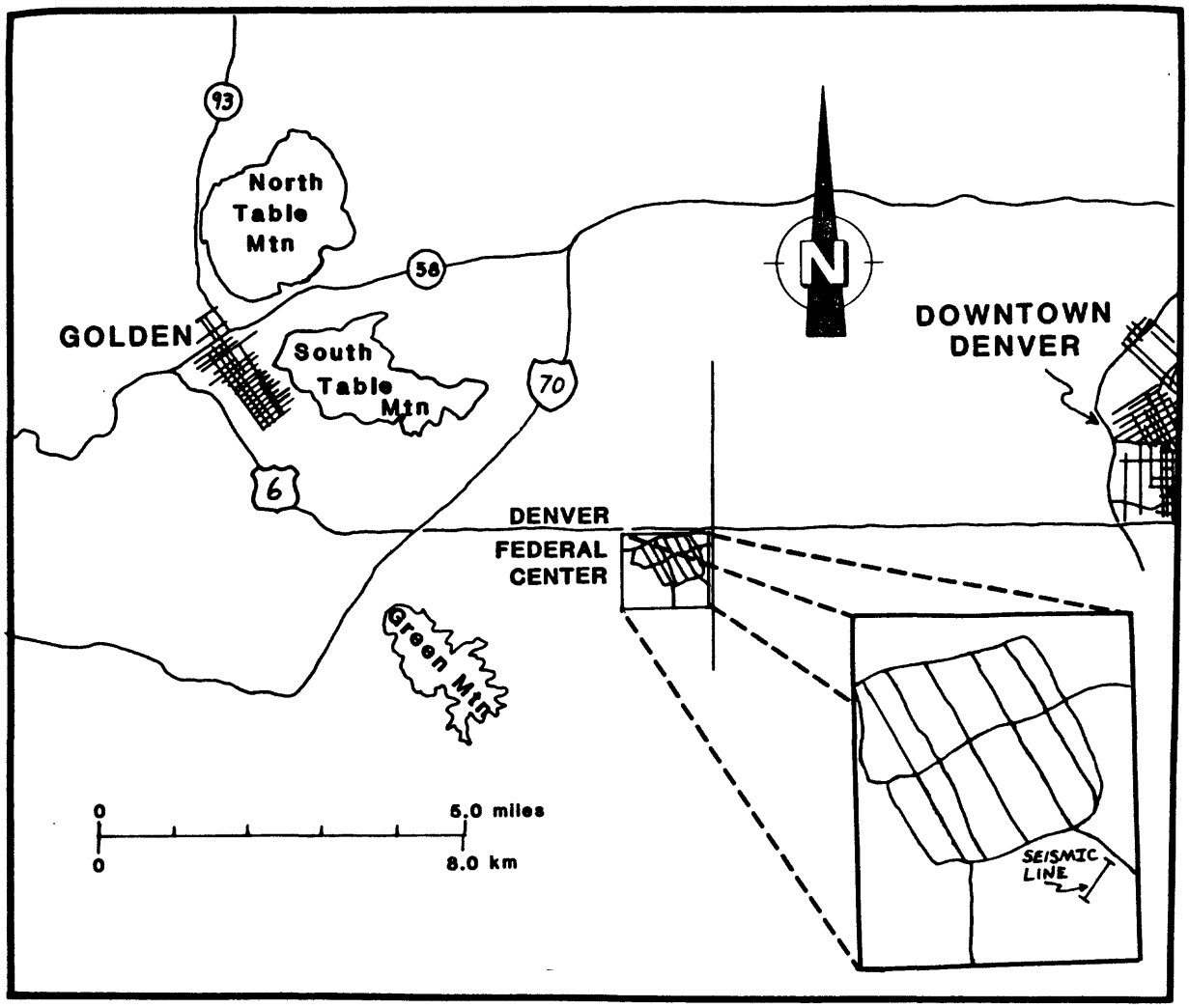

Figure 1.--Map showing location of the Denver Federal Center relative to Denver and Golden, Colo.

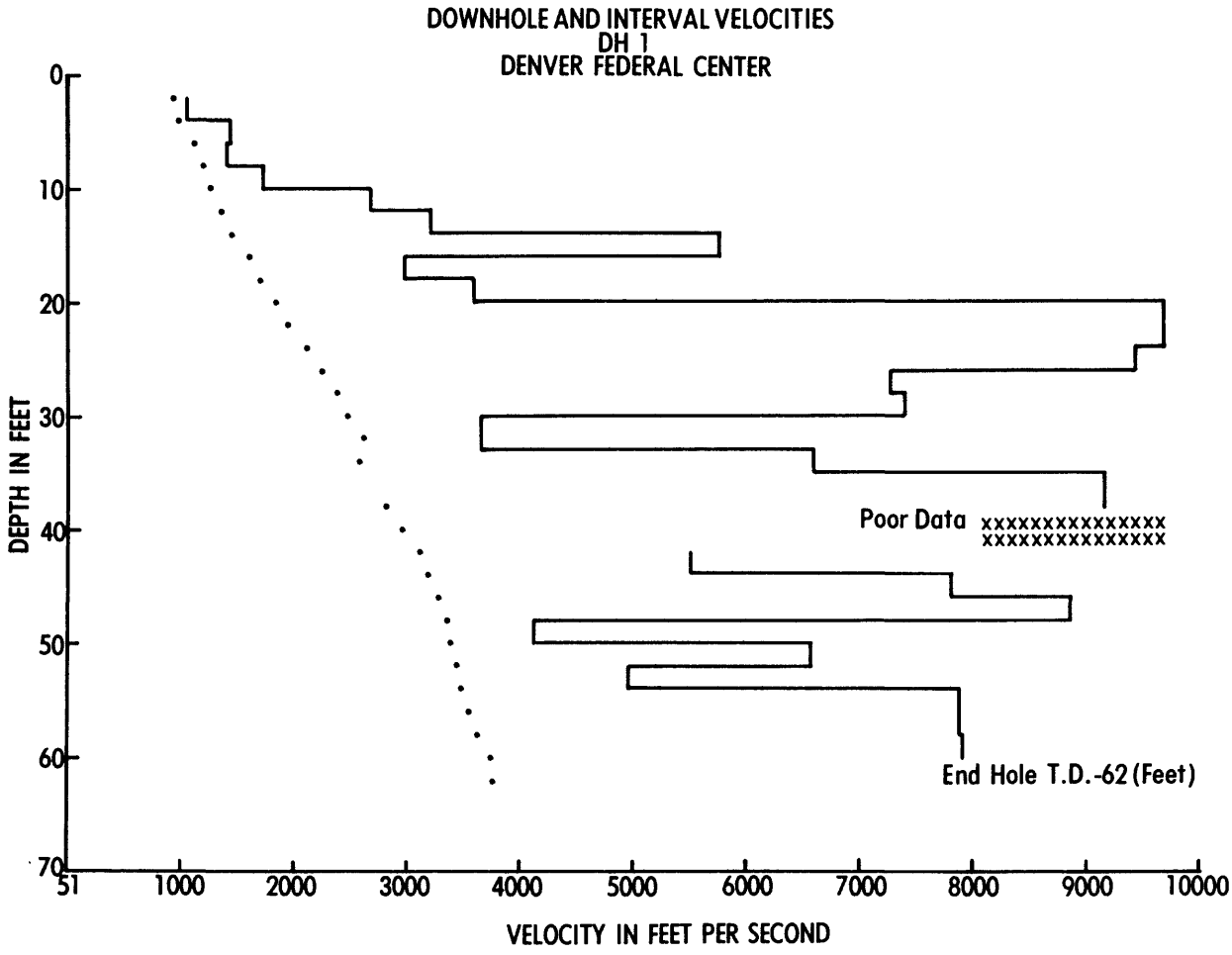

Figure 2.--Average (dots) and interval (solid line) velocities for a drill hole at the Denver Federal Center. Drill hole is located 10 ft from the seismic line.

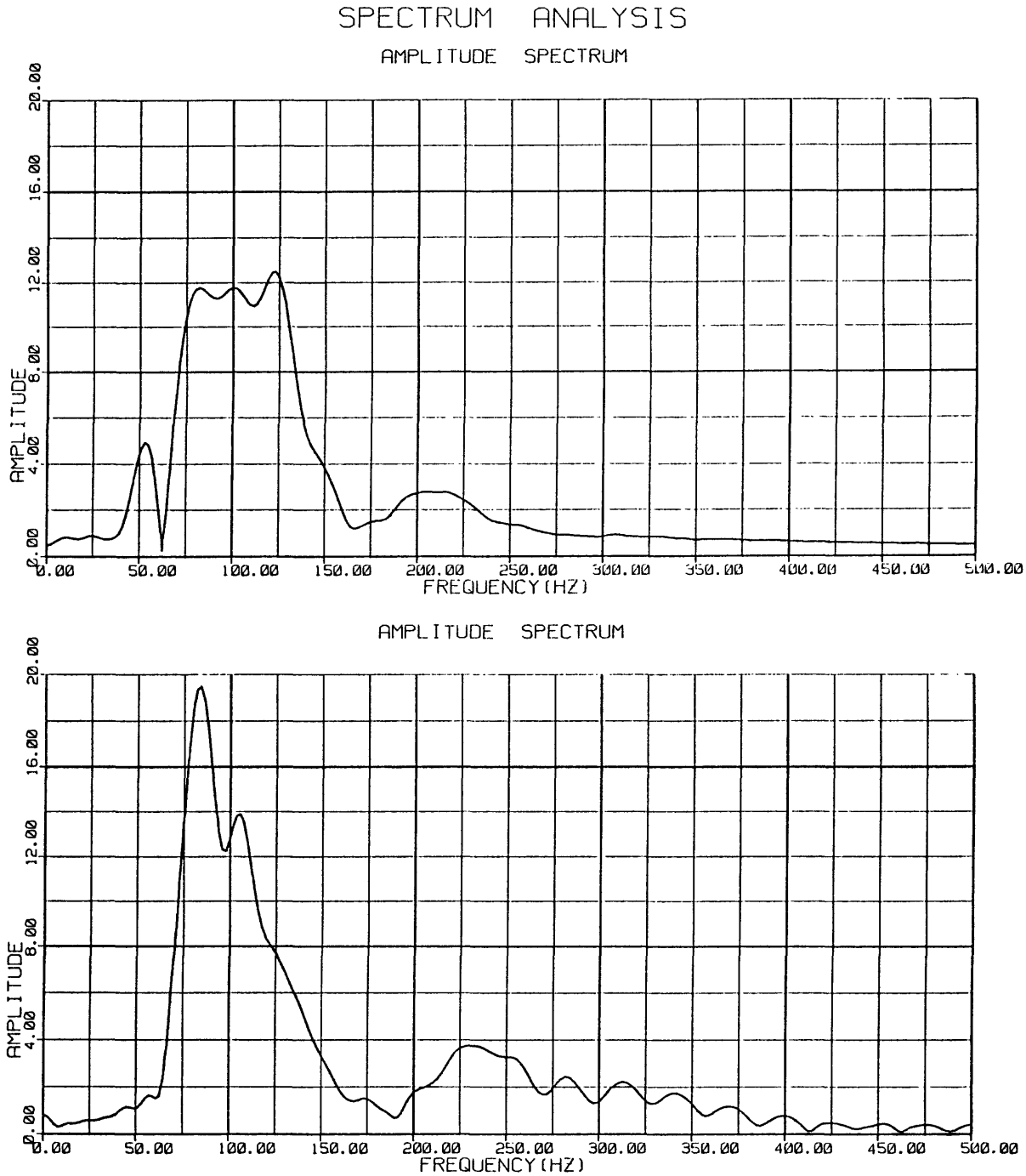

Figure 3.--Amplitude spectra for two unprocessed traces of cdp 148. Upper plot is the spectrum of the nearest trace to the seismic source (10 ft). Bottom plot is the spectrum of the furthest trace from the source (65 ft). Near trace has more low frequency air-blast and ground-roll energy.

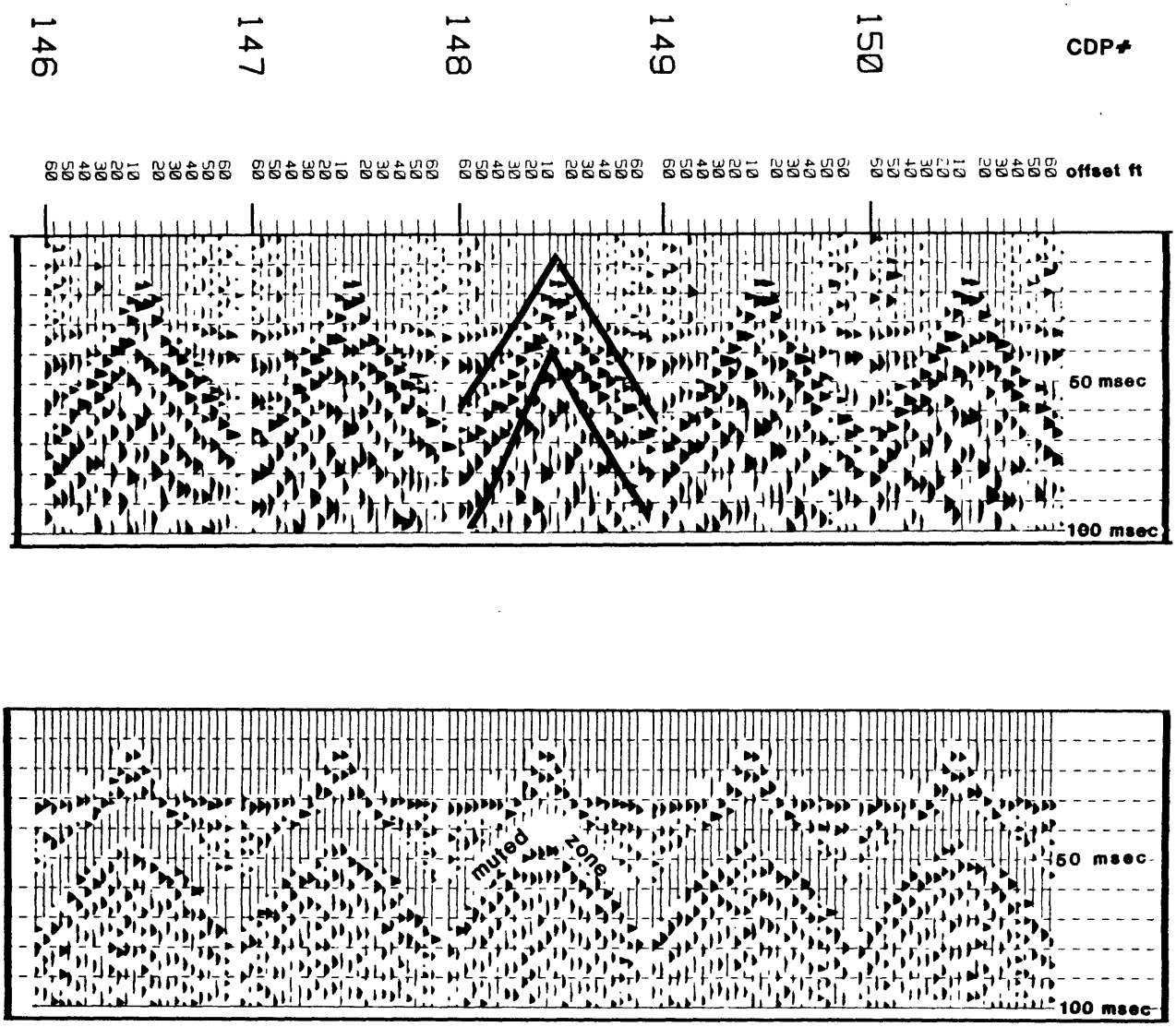

Figure 4.--Upper plot shows 5 consecutive unprocessed 24-fold cdp gathers (except for sorting, editing, and vertical stack). No filtering, nmo correction, or muting has occurred. Note prominent upside-down v-shape expression of the airblast and ground-roll highlighted on cdp 148. Bottom plot shows the same 5 cdp gathers as above, but with nmo, filter, and mute applied. Filtering and muting significantly reduces the influence of airblast and ground-roll energy.

signal suppression outside this pass band) follows all deconvolution tests. This filter band limits the signal output from the deconvolution process because the inverse filter generated in deconvolution is not accurate at very low and very high frequencies where the signal-to-noise ratio is low. In spite of the pre-deconvolution processing steps taken, the data still has a substantial amount of coherent and noncoherent noise which makes it difficult to pick reflections on the cdp gathers. The field and processing parameters are summarized in table 1.

TABLE 1.--Processing sequence and field parameters.

Processing sequence
1. Reformat field data from modified SEG-Y to DISCO format.
2. Trace edit.
3. Vertical stack.
4. Geometry definition.
5. CDP sort.
6. Filter analysis.
7. Velocity analysis.
8. Mute analysis.
9. Pre-stack deconvolution tests.
10. Brute stack.
11. Refine velocities, filters, and mutes.
12. Stack.
13. Post-stack deconvolution tests
14. Final stack.
15. Trace mixing.
16. AGC and plot.

Field parameters	
Instrument type------DHR-2400.	Energy source------12 gauge shotgun.
Tape format----------Modified SEG-Y.	Type projectile---- 1 oz lead slug.
No. channels---------24.	Shots/shotpoint---- 2.
Field filter---------80 Hz high-pass.	Shot interval------ 5 ft.
Fold-----------------24.	Geophone interval-- 5 ft.
Geophone array-------Single, 100 Hz.	Field geometry-----10 ft near offset split spread.

SOURCE SIGNATURE

The source signature for an 8-gauge "Betsy Seisgun" (fig. 5) recorded at a depth of 100 ft from the source shows that it resembles a minimum phase wavelet in character. That is, most of the energy is located in the first part of the wavelet (though some wavelets that are minimum phase do not have this characteristic). The source signature of the 12-gauge gun used for this experiment should be similar to the source signature of an 8-gauge gun. In addition, a dynamite source is known to be minimum phase (Sengbush, 1983);

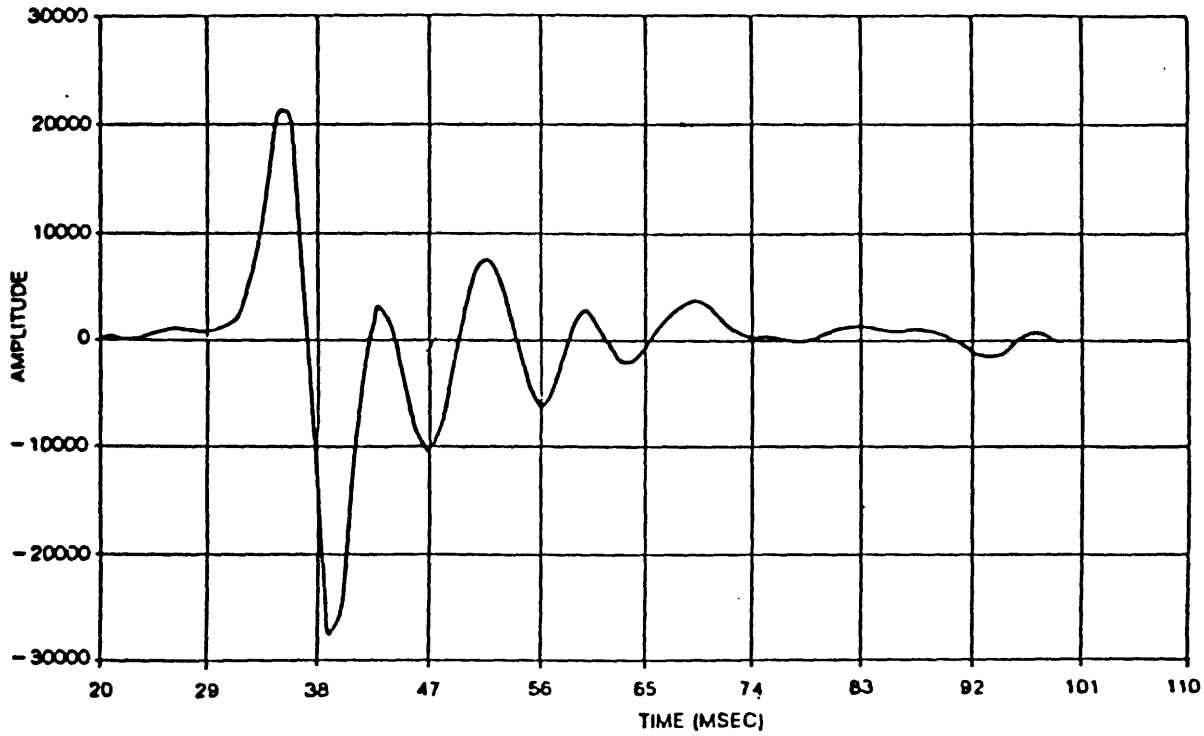

Figure 5.--Betsy 8-gauge shotgun source signature showing the minimum phase character of the wavelet (energy packed at the front of the wavelet). One shot into dry ground. Geophone source sensor located at a depth of 100 ft. Test shot location: Indiana. Figure taken from a Betsy Seisgun pamphlet on operation and performance of the 8-gauge.

therefore, since the shotgun delivers a similar short-duration, highly concentrated impulse, it is reasonable to assume that the shotgun source is minimum phase.

Minimum phase waveforms are an important variable in the Wiener deconvolution process. The Wiener filter methods assume a minimum phase input waveform because of restrictions placed on the waveform by the calculations performed in the generation of the deconvolution filter. Two essential properties of minimum phase wavelets are: (1) they are stable functions and converge quickly, (2) their inverses are minimum phase and therefore stable. Thus, since a Wiener deconvolution process designs an inverse operator to the input data, it is critical that the inverse be a stable function. Minimum phase seismic data satisfies this requirement.

RESULTS

Pre-stack versus post-stack deconvolution.--Performance tests of spiking and gap deconvolution filtering applied before stacking versus after stacking were conducted using data output from the processing stage described previously. Figures 6 and 7 show results of deconvolution filtering applied before and after stacking respectively. The tests reveal a substantial improvement in stack resolution when applying deconvolution after stacking (fig. 7). There are more coherent events, especially in the 20- to 50-ms zone, on the sections which were deconvolved after stacking. Apparently, the stacking process restricted the frequency band, upon which the deconvolution filter was designed, to one that contained more signal and less noise. Others (Jurkevics and Wiggins, 1984; Berkhout, 1977) have found similar results. There is a degradation in deconvolution performance when it is applied in situations of low signal and high noise.

Figures 8 and 9 are the amplitude spectra for deconvolution tests conducted before and after deconvolution respectively. The amplitude spectrums of the same stacked trace from each of the tests above substantiate the claim that data quality improves deconvolving after stacking (figs. 8, 9). These spectra of cdp 148 (100 sample operator lengths, 0.01 percent white noise, and second-zero-crossing gap length) show, for the data which had deconvolution applied after stacking, improved high-frequency enhancement, a smoother spectrum, and a better balance in amplitude among those frequencies in the pass-band as shown in figures 8 and 9.

Comparison of amplitude spectra for spiking and gap deconvolution show their differing responses as well. Spiking deconvolution generates a broader and marginally smoother spectrum. Also, the dominant frequency range is higher for spiking deconvolution. The average frequency for spiking peaks at a higher number than for gap deconvolution.

One advantage of gap deconvolution in this test and in those that follow is that gap deconvolution retains more of the original amplitude level of the data before applying deconvolution. Still, the sacrifice in signal energy using spiking deconvolution in this case can be justified because of the higher resolution stacked trace and frequency enhancement effects mentioned above. Figure 10 shows a direct comparison between deconvolution following stacking versus deconvolution before stacking.

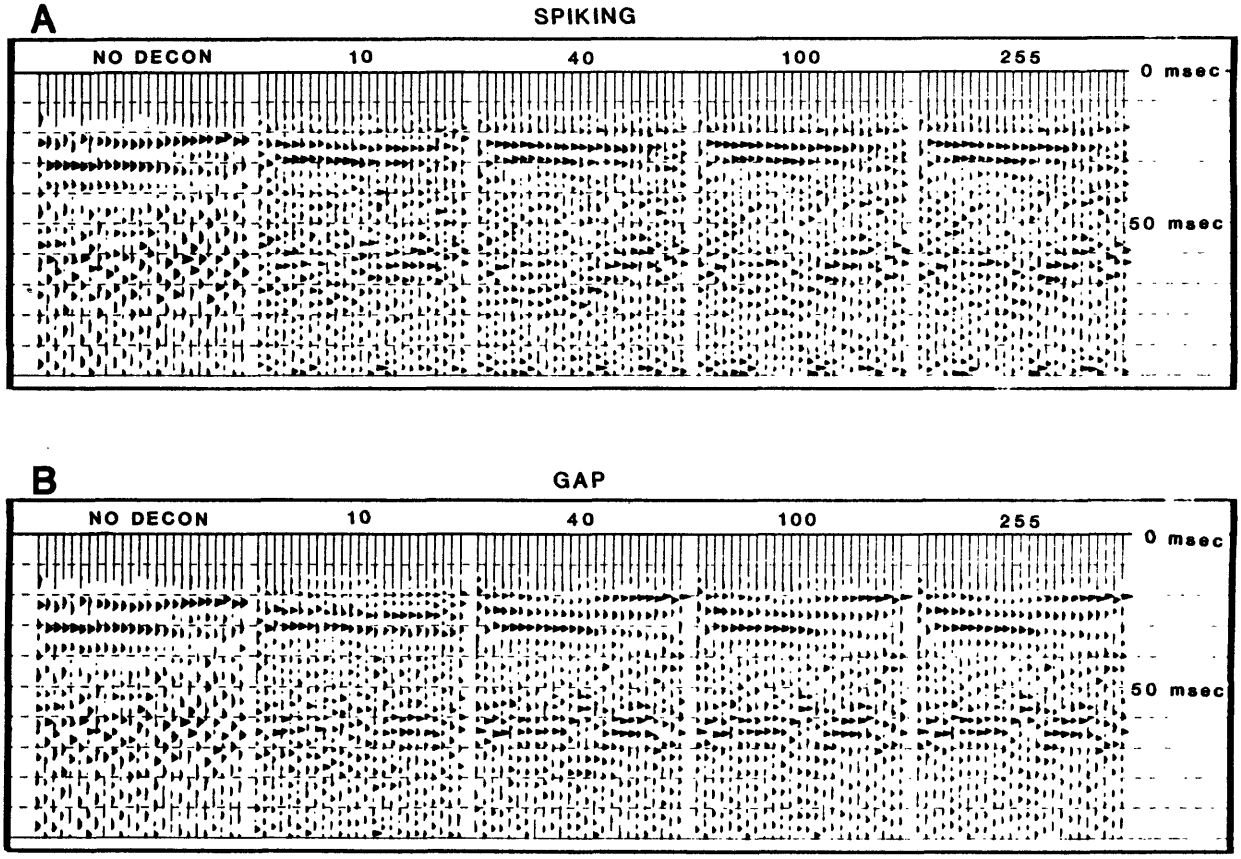

Figure 6.--Results of spiking (A), and gap (B) deconvolution filtering applied prior to stacking. Deconvolution filter operator lengths are indicated at the top of each panel (in sample points). The white noise level was 0.01 percent in all cases. Prediction distance for gap deconvolution was set at the 2nd zero crossing.

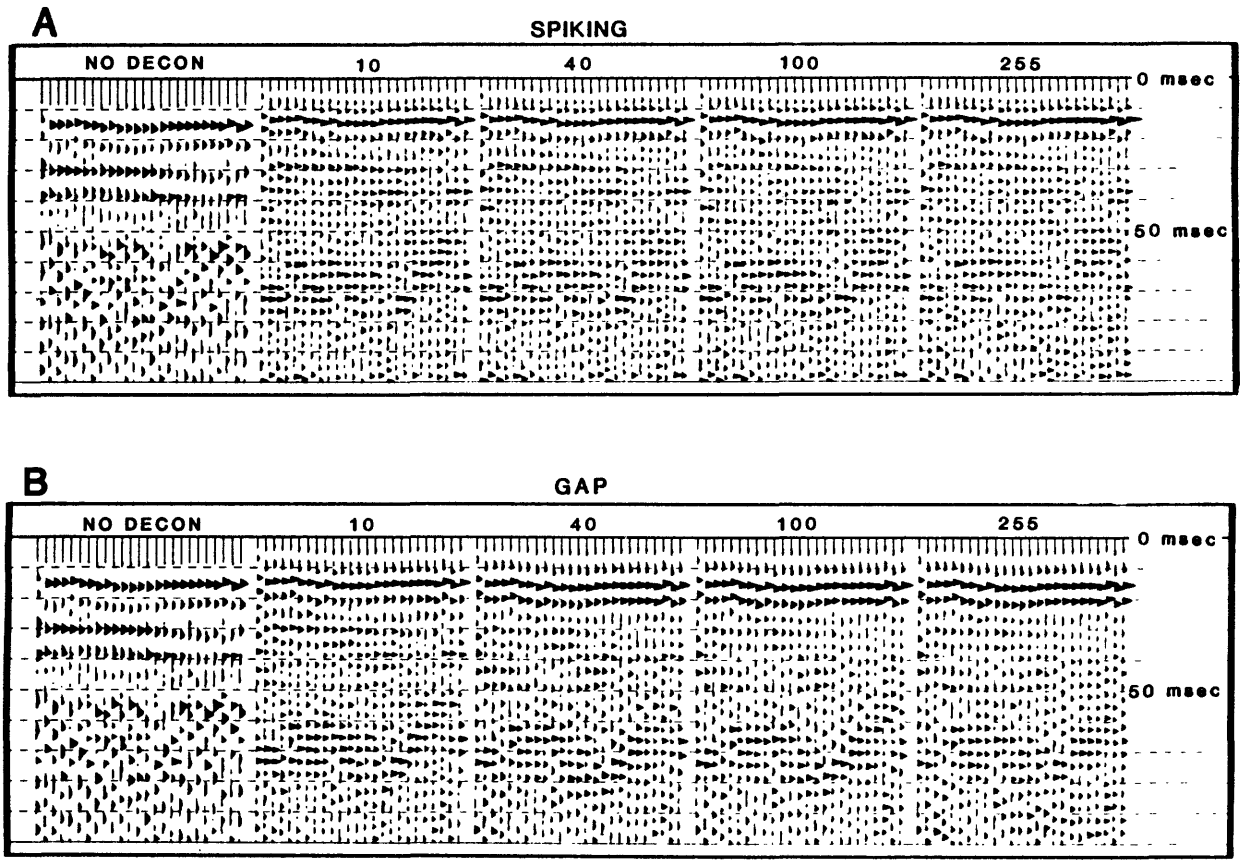

Figure 7.--Results of spiking (A), and gap (B) deconvolution filtering applied after stacking. Deconvolution filter operator lengths are indicated at the top of each panel (in sample points). The white noise level was 0.1 percent in all tests. The prediction distance for gap deconvolution was set at the 2nd zero crossing.

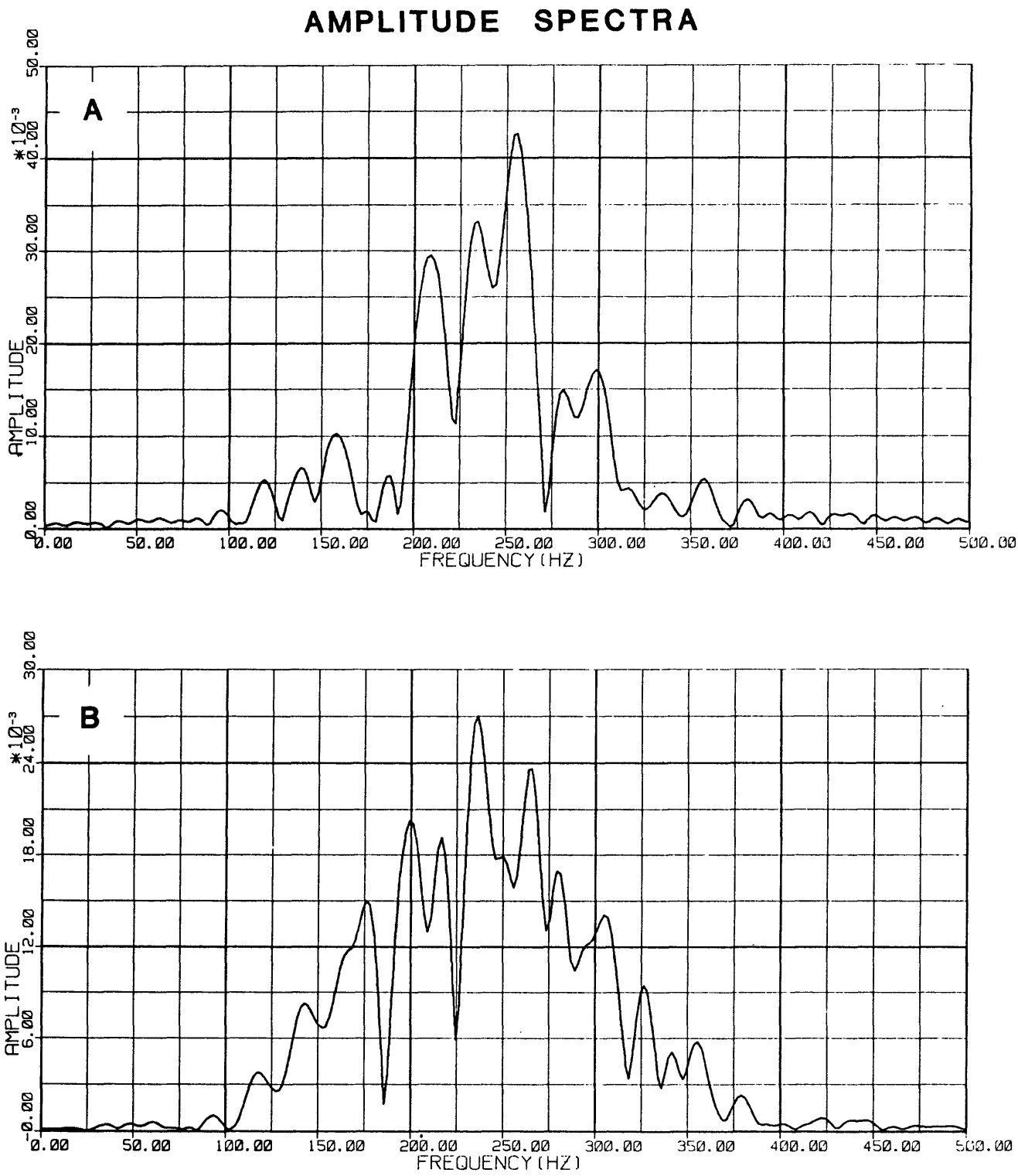

Figure 8.--Spectral analysis comparison for one stacked cdp using spiking deconvolution (A) before stacking and (B) after stacking. Deconvolution parameters in both cases are: 100 sample point operator lengths and a 0.1 percent white noise level.

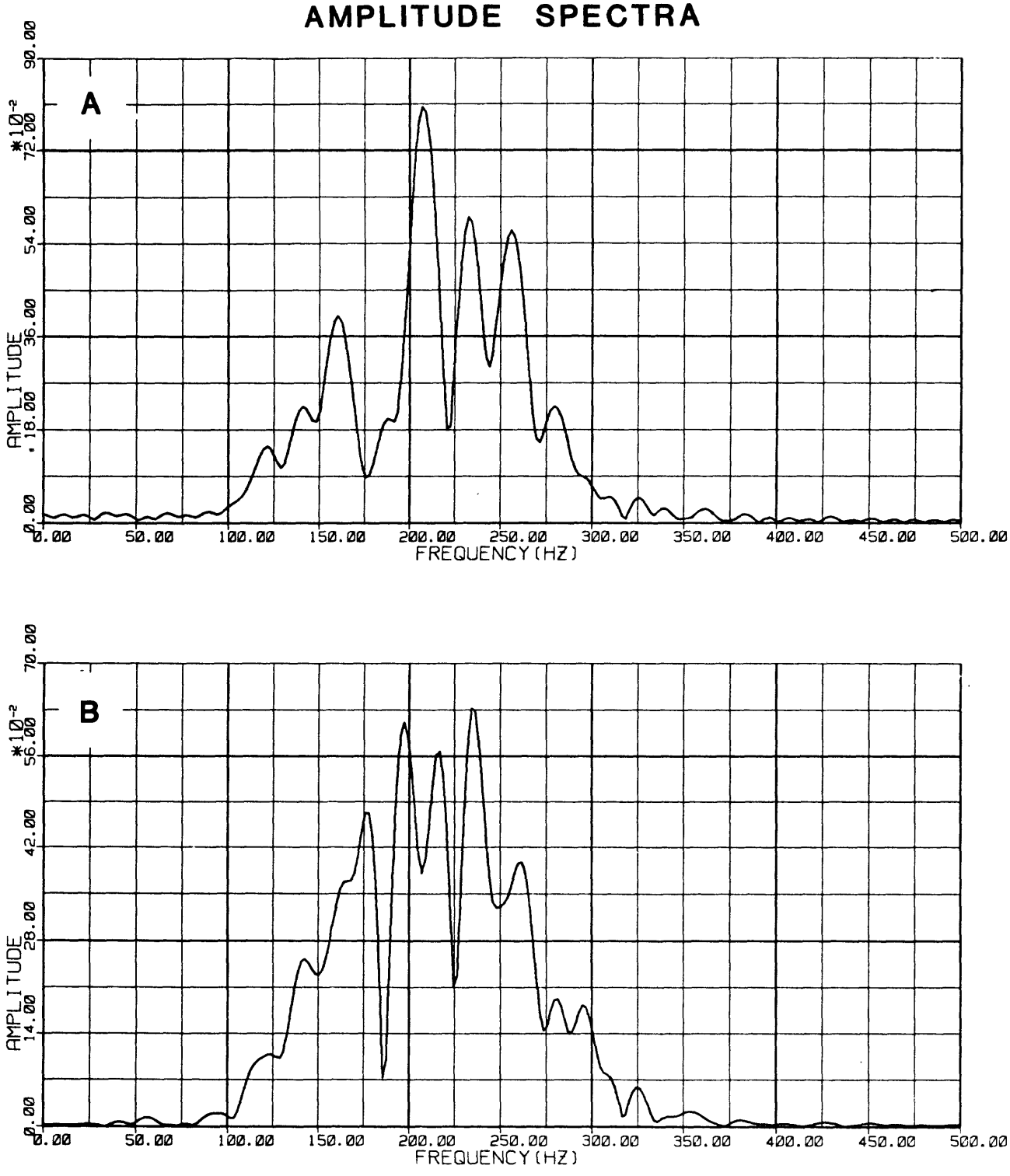

Figure 9.--Spectral analysis comparison for one stacked cdp using gap deconvolution (A) before stacking and (B) after stacking. Deconvolution parameters in both cases are: 100 sample point operator lengths and a 0.1 percent white noise level, and a 2nd zero crossing gap length.

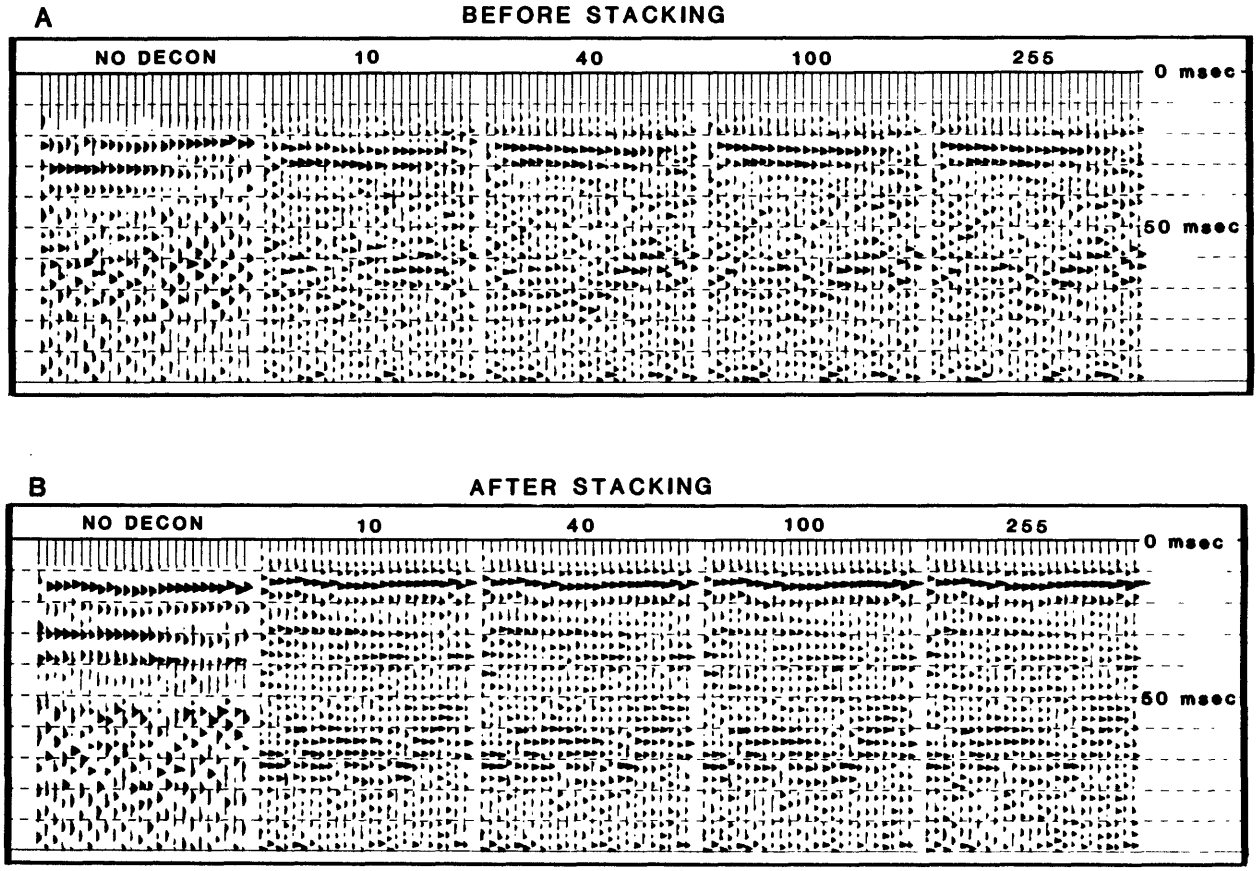

Figure 10.--Comparison of time shifting of reflection events for spiking deconvolution applied (A) before stacking and (B) after stacking. Deconvolution filter operator lengths (in sample points) are annotated at the top of each panel. White noise level for all tests is 0.1 percent.

Time shifting of events.--Figure 7 can also be used to examine two other effects of the deconvolution process: time shifting of reflection events and the insensitivity of stack quality to deconvolution filter operator length.

Berkhout (1977) and Jurkevics and Wiggins (1984) both observed time shifting and phase changes due to increases in white noise level. Deconvolving the field data used in this paper produced time shifts of events for both spiking and gap deconvolution. Deconvolving before stacking caused greater time shifts (2 ms) than when deconvolving after stacking (1 ms) for the event at approximately 30 ms on all panels of figure 10. In the papers by Berkhout and Jurevics and Wiggins mentioned above, time shifting increased as the white noise level increased. Since the stacking process reduces the noise level relative to the signal level, then applying deconvolution prior to stacking as opposed to after stacking would produce data with greater time shifts seen in the reflected events. Notice also that the time shift effect is lessened for gap deconvolution (fig. 7). The smaller time shift observed in gap deconvolution is likely due to the preservation of the original waveform that the gap (prediction distance) length allows.

Filter lengths.--The second effect, observed in figure 7, is the insensitivity of deconvolved stack quality to the length of the filter operator. The operator length for gap and spiking deconvolution varies from 10 samples to 255 samples and shows relatively minor degradation in stack resolution for large increases in operator length. For a 25-fold increase in operator length, there does not appear to be an equivalent magnitude degradation in stack quality. Jurkevics and Wiggins (1984) had a similar result and remarked that the success of the deconvolution operator in generating a spike rests on the proximity of the source wavelet to being minimum phase, and not on operator length. Jurkevics and Wiggins tested nonminimum phase wavelets with different deconvolution filter operator lengths and noted a greater sensitivity between operator length and stack output. This suggests that the field data used in this paper are close to minimum-phase character since the filter operator length had little effect on stack quality.

White noise tests.--Where Jurkevics and Wiggins (1984) and Berkhout (1977) recorded drastic deterioration of stack resolution due to an increase in the white noise level similar tests on this data with white noise as the variable parameter, gave different results. (Adding white noise to the data raises all values on the amplitude spectrum a uniform amount. This procedure prevents the occurrence of an attempt to divide by zero within the deconvolution inverse filter design.) Here, large increases in the white noise level produced minor deteriorating effects on stack quality for deconvolution applied post-stack (figs. 11, 12). For pre-stack deconvolution, adding large amounts of white noise possibly improved the stack, although this is arguable (fig. 13). Jurkevics and Wiggins (1984) and Sengbush (1983) both demonstrated the detrimental effects of adding little (0.01 percent) white noise to the deconvolution process. It remains a puzzle why this data responds as it does to the white noise level variations. Still, the best result with this data was achieved using no white noise, which agrees with the results of the above authors.

Zero-phase filtering.--Figure 14 shows the effect of using the zero-phase band-pass filter before deconvolution. The section on the left (panel A) has

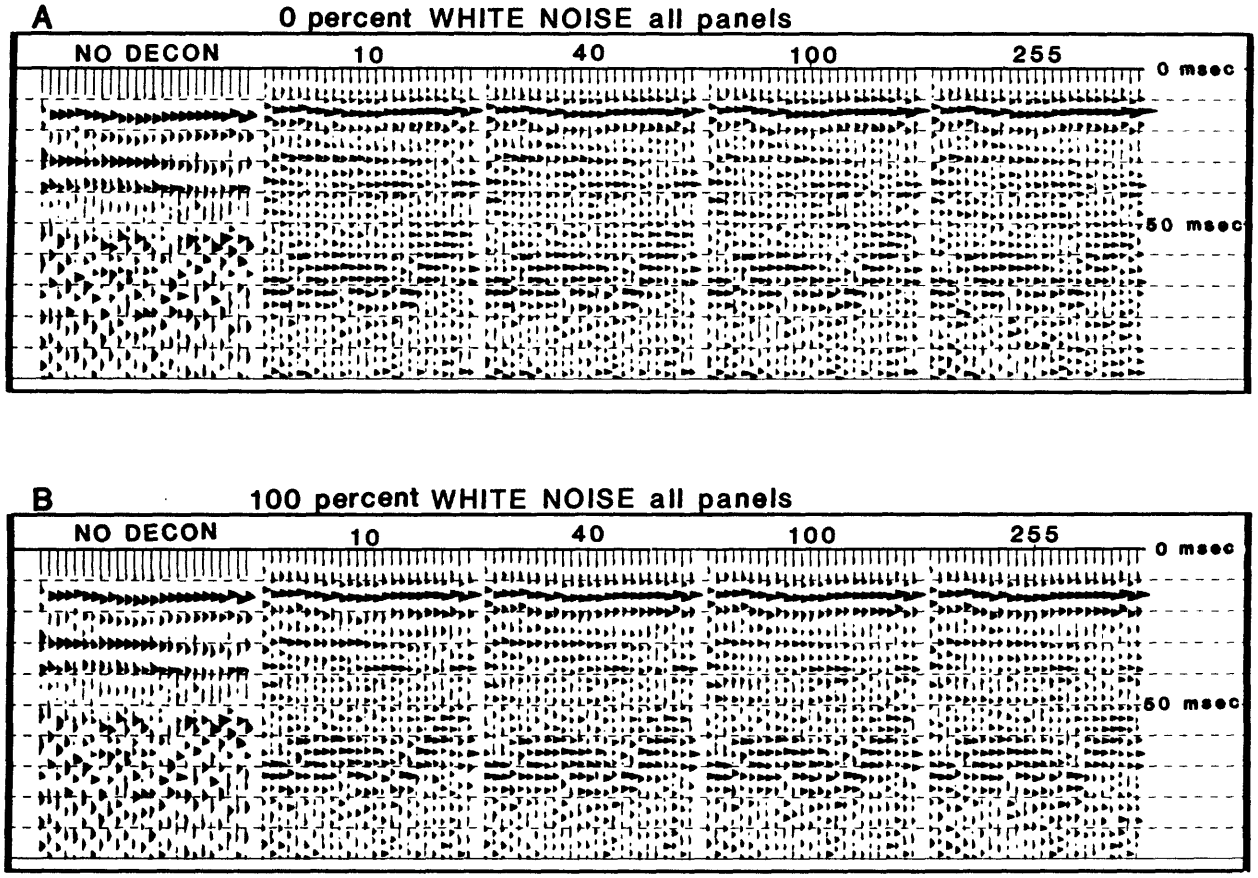

Figure 11.--Results of using spiking deconvolution after stacking (A) without white noise (0.0 percent) and (B) with 100.0 percent white noise. Deconvolution filter operator lengths in sample points are indicated at the top of each panel.

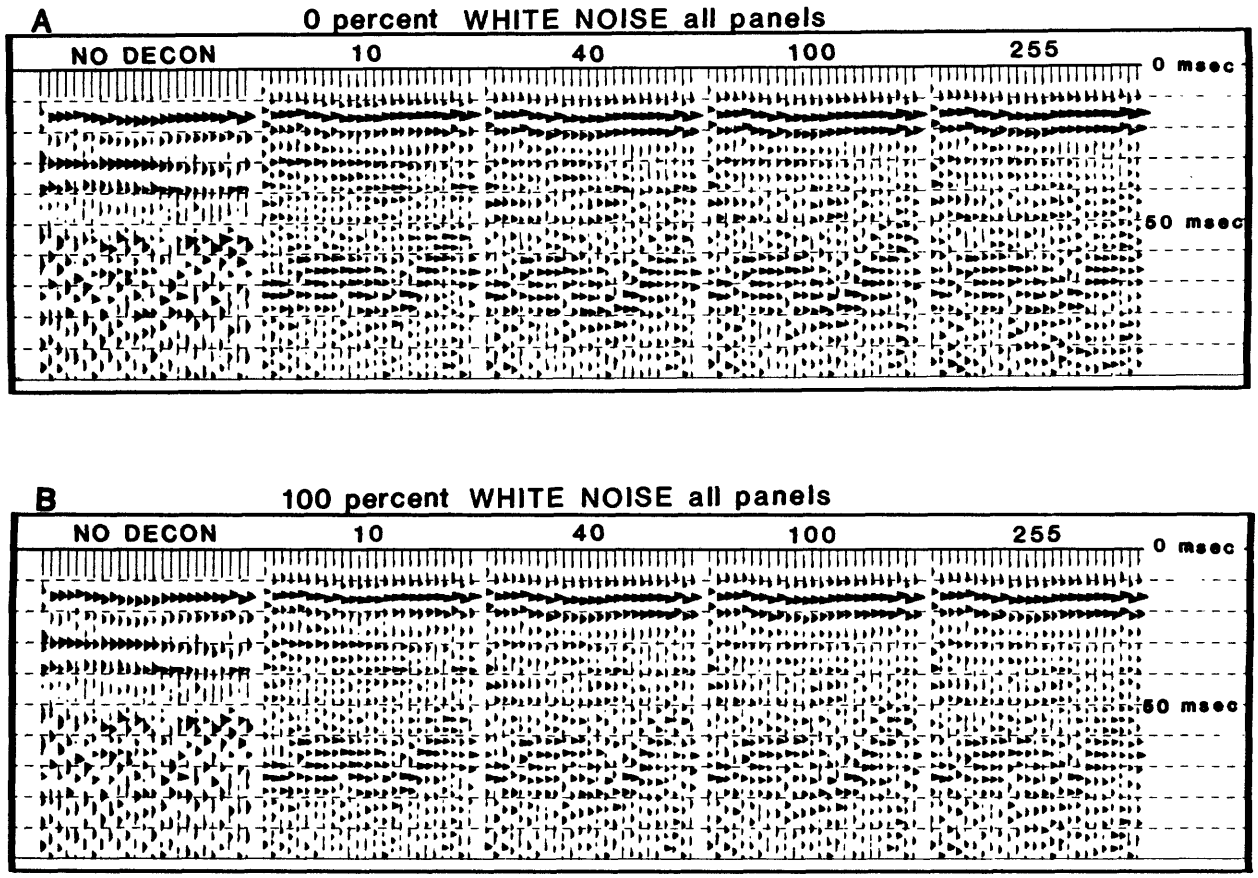

Figure 12.--Results of using gap deconvolution after stacking (A) without white noise (0.0 percent) and (B) with 100.0 percent white noise. Deconvolution filter operator lengths in sample points are indicated at the top of each panel. The gap length is the 2nd zero crossing for all tests.

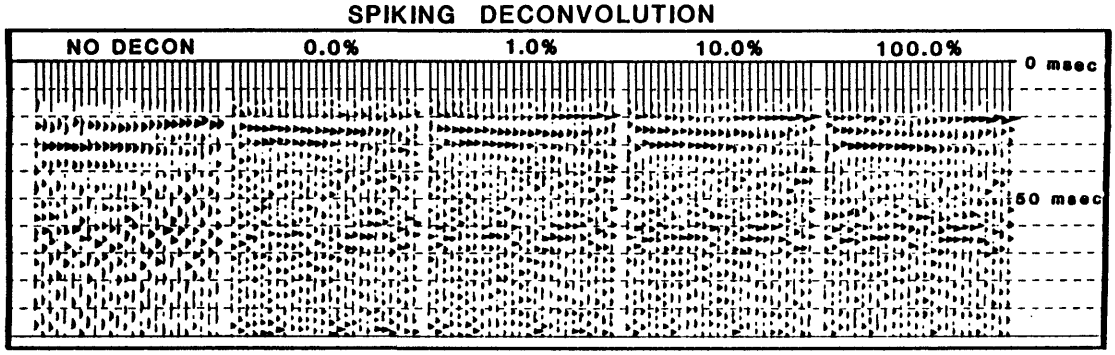

Figure 13.--White noise level tests conducted using spiking deconvolution filtering applied before stacking. Number at the top of each panel indicates the white noise level (in percent) used in running the test on that panel. The deconvolution filter operator length for all tests is 100 sample points.

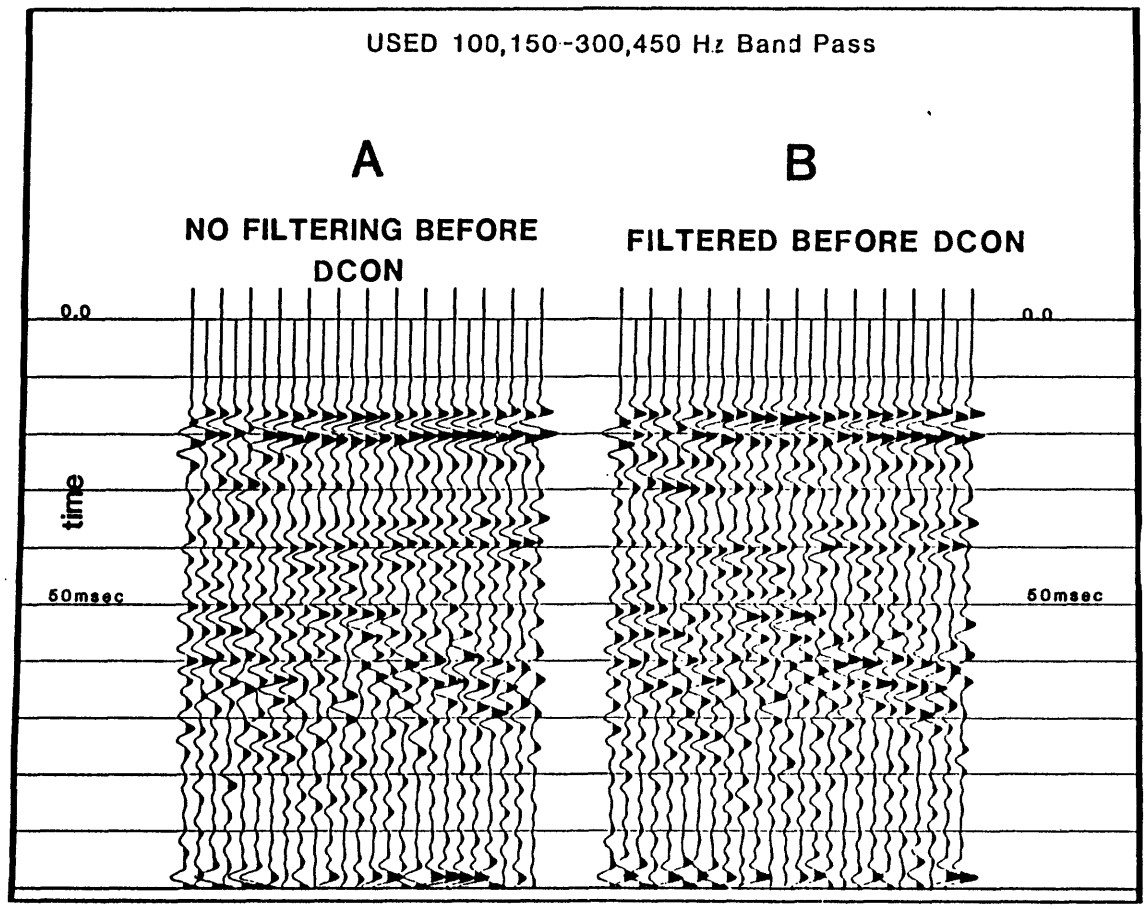

Figure 14.--Results of not using a zero phase filter before spiking deconvolution (A) and (B) with the zero phase band pass filter applied before deconvolution. Deconvolution in both cases occurred after stacking.

the filter applied before deconvolution. The section on the right (panel B) had no filtering prior to deconvolution. Event resolution of panel A is superior to that of panel B down to 33 ms, where the quality of panel B improves and surpasses that of panel A for events down to 50 ms. Subsurface information derived from the well and refraction data can place three different horizons with good confidence at 20 ms, 24 ms, and 31 ms. Using these horizons, one must choose panel A as being superior to panel B, since it resolves these horizons better than panel B.

Zero-phase filtering before deconvolution is not recommended by most authors since it would change minimum phase data to some nonminimum phase form and therefore violate a primary assumption of Wiener deconvolution: that the input seismic data be minimum phase. Berkhout (1977), however, describes a case where zero-phase filtering before deconvolution may be desirable in situations where the data is particularly noisy. The data used in this paper may represent such a case. The raw data is obviously noisy and the deconvolution process gives better results after stack (after noise cancellation?).

Post-deconvolution bandlimiting filter.--Due to the inability of the Wiener process to design a good estimate of the distorted seismic pulse where the signal-to-noise ratio is low, a bandlimiting filter is required following spiking deconvolution (Sengbush, 1983). This filter restricts the bandwidth to the region where there is a higher signal-to-noise ratio. Figure 15 shows five panels of the same stacked data. Panel 1 has no deconvolution for comparison. Panel 2 and 3 have spiking deconvolution applied. Panel 2 displays the results of spiking deconvolution without the following bandlimiting filter. Panel 3 shows the same data as panel 2 except that a bandlimiting filter followed the deconvolution. The presence of enhanced high frequency, not seen on panel 1, shows the spectral restoration effects of spiking deconvolution.

Gap deconvolution, on the other hand, uses prediction distance as a built-in bandlimiter (Sengbush, 1983). The prediction distance preserves the waveform up to the time specified by the prediction distance. This procedure effectively reduces or eliminates the need to apply another bandlimiting filter following deconvolution. Panel 4 and 5 of figure 15 show the built-in bandlimiting feature of gap deconvolution quite well. The data in panel 4 was displayed without the filter following deconvolution while panel 5 displays the same data with the filter applied after deconvolution. Notice the narrower bandwidth of panel 4 as compared to that of panel 2.

Subsurface modeling.--Additional subsurface data acquired through refraction and down-hole techniques help constrain the velocity and depth models for this seismic line. Figure 16 was derived using Geoquest International AIM's package. Convolving a synthetic zero-phase source pulse over the reflectivity determined from refraction and boring data produced a synthetic stack (fig. 16A). Strong velocity contrasts at 12, 14, and 35 ft generate reflections at 20, 24, and 30 ms, respectively. Figure 16B is a stacked seismic field section, with spiking deconvolution applied post-stack, showing how well the deconvolution process has resolved these events. The event at approximately 17 to 18 ms is an artifact of the filter convolution process as it operates on some low-energy noise.

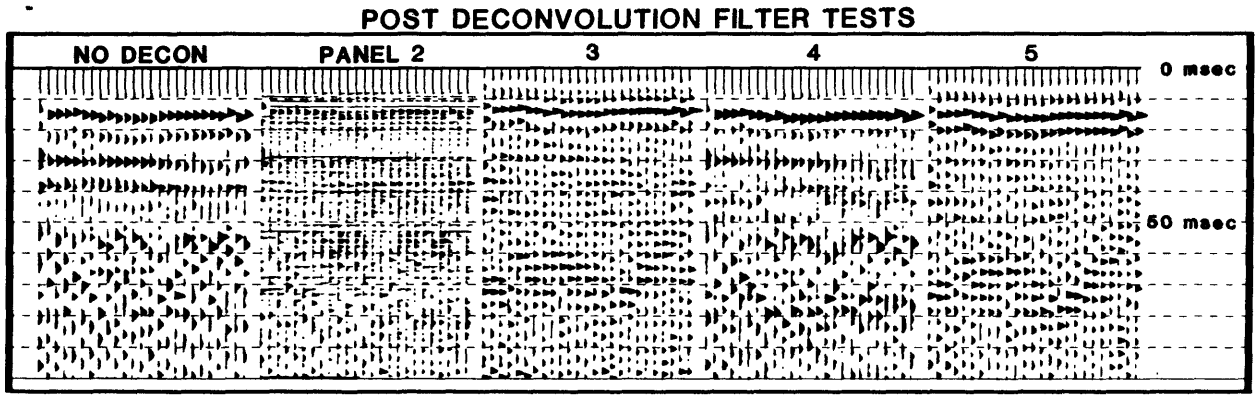

Figure 15.--Results of zero-phase filtering after deconvolution. Spiking deconvolution applied after stacking without the post-deconvolution filter (panel 2) and (panel 3) with the post-deconvolution filter. Gap deconvolution applied after stacking without the post-deconvolution filter. The white noise level is 0.1 percent and the deconvolution filter operator is 120 sample points for all tests. Gap distance was the 2nd zero crossing.

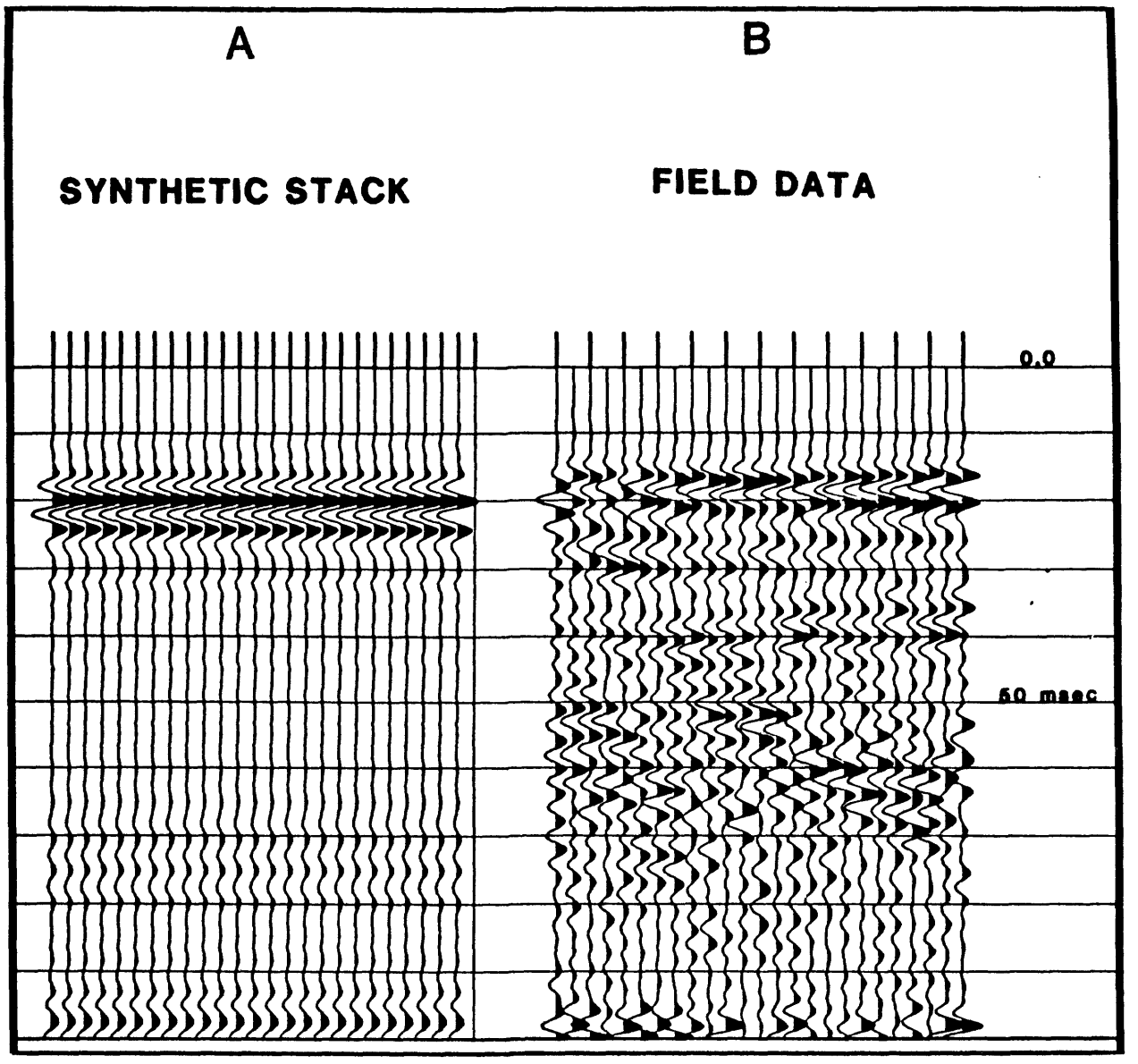

Figure 16.--Comparison of synthetic stack (A) to (B) the real field data. Spiking deconvolution was applied after stacking (10 sample operator length and 0.0 percent white noise) in (B).

CONCLUSIONS

Several tests of Wiener spiking and predictive (gap) deconvolution were evaluated using short record length reflection field data. Applying spiking and gap deconvolution after stacking gave better results than using them before stacking. The performance of spiking and gap deconvolution were similar, but spike filtering showed slightly better spectral broadening and smoothing characteristics than did gap filtering. Time shifting of reflection events was found to be more severe using spike (1-2 ms versus 0-1 ms) than gap filtering. Stacked data quality was found to be relatively insensitive to filter operator length for both spiking and gap deconvolution. What one would have thought to be an excessive level of white noise added to the data produced minor degrading effects on stack quality. Zero-phase filtering before deconvolution proved beneficial to stack resolution for the upper 35 ms, while deconvolved data without the prior filter was superior for the remainder of the section. The effect of post-deconvolution filters was examined and compared for spiking and gap deconvolution, demonstrating that it was more important and critical for spiking. Finally, a depth model generated from data collected through refraction and well surveys showed a good correlation to the deconvolved seismic field records.

In summary, the goals of deconvolution for regular length seismic records (3-6 s) used in the seismic data processing industry of (1) spectral equalization, (2) spectral whitening, and (3) improved resolution (SEG Research Committee, 1985), have been shown to be reasonable objectives for this short record length (100 ms) data as well. Although there were some rather odd results, such as the effect of excessive white noise levels and zero-phase filtering before deconvolution, Wiener deconvolution is still effective in reaching these goals. Therefore, this test of processing techniques shows the possibilities of improving the resolution of near-surface structures (faults, alluvial thicknesses over bedrock) encountered in applications of shallow seismic reflection profiling to engineering geology.

REFERENCES

Berkhout, A. J., 1977, Least squares inverse filtering and wavelet deconvolution: Geophysics, v. 42, no. 7, p. 1369-1383.

Jurkevics, Andrejs, and Wiggins, Ralphe, 1984, A critique of seismic deconvolution methods: Geophysics, v. 49, no. 12, p. 2109-2116.

SEG Research Committee, 1985, Seismic deconvolution workshop: Geophysics, v. 50, no. 4, p. 715-735.

Sengbush, R. L., 1983, Seismic exploration methods: Boston, Mass., International Human Resources Development Corporation, 296 p.